

# CHARACTERISTICS OF STRESS-INDUCED TRANSFORMATION AND MICROSTRUCTURE EVOLUTION IN Cu-BASED SMA<sup>\*\*</sup>

Cheng Peng    Xingyao Wang    Yongzhong Huo<sup>\*1</sup>

(Department of Mechanics and Engineering Science, Fudan University, Shanghai 200433, China)

Received 29 October 2007, revision received 26 January 2008

**ABSTRACT** The mechanical behavior of shape memory alloys (SMAs) is closely related to the formation and evolution of its microstructures. Through theoretical analysis and experimental observations, it was found that the stress-induced martensitic transformation process of single crystal Cu-based SMA under uniaxial tension condition consisted of three periods: nucleation, mixed nucleation and growth, and merging due to growth. During the nucleation, the stress dropped rapidly and the number of interfaces increased very fast while the phase fraction increased slowly. In the second period, both the stress and the interface number changed slightly but the phase fraction increased dramatically. Finally, the stress and the phase fraction changed slowly while the number of interfaces decreased quickly. Moreover, it was found that the transformation could be of multi-stage: sharp stress drops at several strains and correspondingly, the nucleation and growth process occurred quasi-independently in several parts of the sample.

**KEY WORDS** stress-induced martensitic transformation, CuAlNi single crystal, microstructure, nucleation, growth

## I. INTRODUCTION

Shape memory alloy (SMA) is an important active material and has found many applications due to its shape memory effect and superelasticity<sup>[1-4]</sup>. With the fast development of sputtering and micro manufacturing technology, SMA is considered as an ideal candidate for actuating components in MEMS<sup>[5-7]</sup>. It has been known that SMAs' unique mechanical behaviors are due to the thermal-mechanical coupling resulted from the martensitic transformation<sup>[5,8]</sup>. And during the transformation, fine layered microstructures were often observed and their evolution is closely related to the macroscopic mechanical behaviors, especially the nonlinear phenomena such as instability and hysteresis<sup>[9,10]</sup>. Therefore, for the understanding and modeling of the multi-scale effect it is important to study the microstructure evolution and its relation to the macroscopic behavior.

The superelastic behavior of SMA has been well studied experimentally. It was reported that numerous martensitic strips could appear, and as the loading proceeded, the strips grew up and merged into larger ones, until the martensitic transformation finished and the whole sample was in martensite phase. Correspondingly, the stress-strain relation was linear elastic before and after the transformation, while exhibited a stress plateau during the transformation and a stress-strain hysteresis after unloading<sup>[11]</sup>.

\* Corresponding author. E-mail: yzhuo@fudan.edu.cn

\*\* Project supported by the National Natural Science Foundation of China (Nos. 10372033 and 10672042), Pujiang Scholar Program and Natural Science Foundation of Shanghai (No. 06ZR14009).

However, unlike the quantitative measurement of the stress-strain relation, most of the illustrations of the microstructures are mainly qualitative and often local<sup>[9-12]</sup>. This makes it very difficult to quantitatively analyze the coupling relationship between the microstructures and the mechanical behaviors, and to test the multi-scale models of the phase transition process.

In this paper, the stress induced martensitic transformation of CuAlNi single crystalline SMAs was studied under uniaxial tensile loading-unloading tests. Using the image processing technique and statistical analysis method, quantitative information of microstructures was obtained. Thus it is possible to describe the microstructure evolution of the whole sample during the loading process and to further understand its relation with the stress-strain curve.

Theoretical study<sup>[13]</sup> showed that SMA has the characteristics of first order phase transformation, nucleation and growth under uniaxial loading. Stress drop accompanied with the appearing of thin martensitic strips would occur during the nucleation, while the growth of martensitic strips can also be accompanied with nucleation of new martensitic strips. The number of martensitic strips (which can be represented by the number of interfaces) increases and then decreases during the whole loading process. The range of the stress drop and the maximum number of interfaces are determined mainly by the interfacial energy between martensite and austenite, as well as the inhomogeneous energy due to boundary restrictions.

In this paper, based on the small parameter approximation of the energy function of SMA under uniaxial tension, a new energy function, which is very similar as that in Ref.[13], was obtained. From this new function, the characters of the nucleation and growth were analyzed theoretically. The mechanical behaviors and the microstructure evolution of CuAlNi single crystalline SMAs were studied under uniaxial tensile loading-unloading tests. The surface of the samples was observed simultaneously under an optical microscope. Digital images were taken to cover the whole specimen. Using the photo processing technique and statistical analysis, quantitative information of the microstructures was obtained. The number of the martensitic strips (the number of interfaces), their total width (the phase fraction) and their changing details along the sample can also be obtained. Experimental results showed that the stress-induced martensitic transformation process in single crystal Cu-based SMAs under uniaxial tension conditions consisted of three periods: nucleation, mixed nucleation and growth, and merging due to growth. During the nucleation, the stress dropped rapidly and the number of martensitic strips (the number of interfaces) increased very fast while total width of the martensitic strips (the phase fraction) increased slowly. In the mixed nucleation and growth period, both the stress and the number of the martensitic strips (the number of interfaces) changed slightly but the total width of martensitic strips (the phase fraction) increased remarkably. Finally in the merging due to growth period, the stress and the total width of the martensitic strips (the phase fraction) changed slowly while the number of the martensitic strips (the number of interfaces) decreased quickly. Moreover, from the number of interfaces and the phase fraction along the whole sample during the loading process, it was found that the transformation had a multi-stage characteristics. On one hand, there were several stress drops at different strains in the stress-strain curve; on the other hand, far from the previous nucleation and growth areas, the martensitic transformation could take place with the three-period characteristics as well. In particular, the nucleation of martensitic strips was accompanied with a sharp stress drop. Further study indicated that the sample could be divided into several quasi-independent parts along the tensile direction. In each part, the transformation of three-period would occur independently, and the nucleation would be accompanied with stress drop. Moreover, the relation between the number of interfaces and the phase fraction had very similar characteristics in all parts and could be fitted quite well with theoretical prediction.

## II. ENERGY FUNCTION MINIMIZATION DURING THE STRESS INDUCED MARTENSITIC TRANSFORMATION

Numerous theoretical studies<sup>[14-18]</sup> on the martensitic transformation of SMAs were carried out, and the energy function of the martensitic transformation under uniaxial loading can be described as the following<sup>[14]</sup>,

$$F(u) = \int_0^L \left[ W(u_x, T) + \frac{1}{2} \alpha u_{xx}^2 + \frac{1}{2} \beta (u - u_H)^2 \right] dx \quad (1)$$

where  $L$  is the length of the specimen,  $u(x)$  is the uniaxial displacement field,  $W(u_x, T)$  denotes the free energy density,  $\alpha > 0$  is the coefficient of the strain gradient dependent interfacial energy,  $\beta > 0$  is the coefficient of the displacement dependent inhomogeneous energy, and  $u_H(x) = u(0) + [u(L) - u(0)]x/L$  is the corresponding homogeneous displacement. In order to describe the martensitic transformation, the free energy density  $W(u_x, T)$  should be a non-convex function. In the superelastic case, it can be a piecewise quadratic function<sup>[19]</sup>,

$$W(\varepsilon, T) = \begin{cases} f_A^0(T) + \frac{1}{2}E\varepsilon^2, & \text{Martensite} \\ f_M^0(T) + \frac{1}{2}E(\varepsilon - \varepsilon_m)^2, & \text{Austenite} \end{cases} \quad (2)$$

where  $f_A^0(T)$  and  $f_M^0(T)$  are the chemical energy of the austenite and the martensite at the temperature  $T$ , respectively.  $E > 0$  is the Young's modulus (they are nearly equal in the two phases), and  $\varepsilon_m > 0$  is the transformation strain (about 6%~8%).

Because of the non-convex energy function, it is hard to solve the problem by energy function minimization<sup>[20]</sup>. An applicable way is the small parameter approximation, which means that when the coefficients of interface energy and inhomogeneous energy are small, the energy density function  $f = F/L$  can be simplified into the following energy function,

$$f(\varepsilon, N, Z) = Zf_M^0(T) + (1 - Z)f_A^0(T) + \frac{1}{2}E(\varepsilon - Z\varepsilon_m)^2 + \tau_1 \frac{N}{L} + \frac{\tau_2}{2} \left[ \frac{Z(1 - Z)}{N/L} \right]^2 \quad (3)$$

where  $\varepsilon = [u(L) - u(0)]/L$  is the total strain,  $Z$  is the percentage of martensite phase (phase fraction), and  $N$  is the number of interfaces between the martensite and the austenite. The effective coefficients of interface energy and inhomogeneous energy are

$$\tau_1 = \frac{5}{2}\sqrt{E\alpha}\varepsilon_m^2, \quad \tau_2 = \frac{2}{3}\beta\varepsilon_m^2 \quad (4)$$

In Ref.[13], the energy function very similar to Eq.(3) was obtained. However, the chemical energy was not considered and the Eq.(4) was not obtained. Through the minimization of the energy function Eq.(4) with respect to  $N$ , the relation between the number of interfaces and the phase fraction can be obtained as

$$n(Z) = N/L = n_{\max} [4Z(1 - Z)]^{2/3} \quad (5)$$

$$n_{\max} = \left( \frac{1}{60} \frac{\beta}{\sqrt{E\alpha}} \right)^{1/3} \quad (6)$$

where  $n_{\max}$  is the maximum number of interfaces per unit length. Obviously, small coefficient of interfacial energy  $\alpha$  and/or large coefficient of inhomogeneous energy  $\beta$  induce more interfaces. And because of the infinite derivative at the point  $Z = 0$  in Eq.(5), there should be a nucleation barrier at the beginning of the martensitic transformation. And consequently, finite number of martensitic strips could form and a stress drop would occur<sup>[13]</sup>. In the following experimental section, the effect of the parameters on the microstructures will be discussed in detail.

### III. OBSERVATION OF THE STRESS INDUCED MARTENSITIC TRANSFORMATION PROCESS

#### 3.1. Experimental Procedures

##### 3.1.1. Material preparation and experimental set-up

Six tensile specimens were cut from a CuAlNi (Cu-13.19Al-4.43Ni (wt %)) shape memory alloy single crystal ingot (26 mm in diameter and 70 mm in length) along the length direction and parallel with each other, using a wire-cutting electrical discharge machine. The shape and size of the specimens are shown in Fig.1, and the thickness of the specimen is 0.8 mm. Then the specimens were heat treated at 1073 K for 20 minutes and then quenched into 393 K oil, cooling down to room temperature. The transformation temperatures ( $M_s = 228$  K,  $M_f = 223$  K,  $A_s = 250$  K,  $A_f = 256$  K) were measured by differential scanning calorimeter (DSC). The experiments were conducted at  $T = 293$  K on a self-designed loading device under displacement control loading condition, and the strain rate is kept slowly at about  $2 \times 10^{-5} \text{ s}^{-1}$ . The grips are so designed that the two ends of the specimen cannot move in the transversal direction.

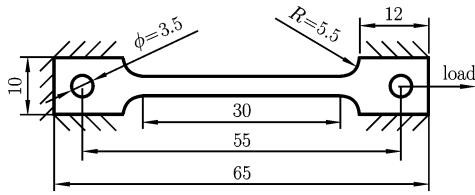


Fig. 1. Shape and size of the CuAlNi single crystal, thickness= 0.8 (unit: mm).

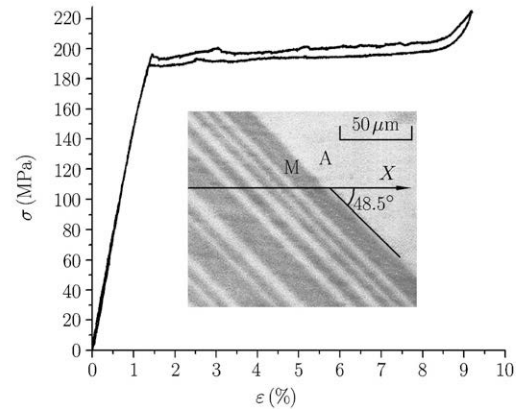


Fig. 2. Stress-strain curve and microstructures during stress induced martensitic transformation.

### 3.1.2. Observation of the microstructures evolution during the martensitic transformation

All specimens were hand-polished in order to observe the changeable microstructures by optic microscope. The microstructures evolution can be recorded either by video camera or photo camera. But in order to get the quantitative information, the digital images of the specimen surface were taken, processed and analyzed by the following procedure. First, the loading process was stopped at preselected strain values and several images were taken. A magnification of 200 was chosen to ensure a clear view and enough resolution for further images processing and analysis. Totally 35 photos were taken along the specimen so to cover the total length. Secondly, the 35 photos were patched up consecutively and the final image of the whole sample was obtained. From different final images taken at different strain values, the microstructure evolution can be studied and analyzed.

### 3.1.3. Image analysis of the microstructures and the phase character function

Since the colors of the martensite and the austenite layers were different, just as in the middle of Fig.2, the image of the whole sample was first transformed into a black-white image (while the black regions for the austenite and the white ones for the martensite). Then, the black-white image was further transformed into a digital matrix  $M$  in which each element equals either zero or one (while zero represents the white color and one represents the black color) so that the martensite/austenite strips can be easily distinguished and divided. Because of the fine layered microstructures, the two-dimensional case in the specimen surface was then simplified into the one-dimensional case. In this way, the values of one line in the matrix  $M$  could represent the whole information of the microstructures along the tensile direction. From these characteristics of the microstructures, the phase character function  $\chi(x, t)$  was defined (while value zero represents the austenite and one represents the martensite).

### 3.1.4. Statistical analysis of the microstructures: the number of interfaces and the phase fraction

In principle, all the information of the microstructure evolution was documented by the phase character function  $\chi(x, t)$  obtained from the digital matrix at various positions of the loading-unloading process. However, just as shown in Fig.2, when the martensitic strips were too thin, the function  $\chi(x, t)$  was highly oscillating in the  $x$  direction and was very difficult to be directly analyzed. Instead, certain kinds of statistical average should be examined to obtain detailed information of the transformation process.

In order to describe the characteristics of the number of interfaces and the percentage of martensite, two important functions were used: the function of the number of interfaces and the function of the phase fraction. They were obtained by the following method: First,  $N(t)$ , the function of the number of interfaces between the martensite and the austenite was obtained by counting the number of locations in the phase character function  $\chi(x, t)$  where the value changes from zero to one or one to zero (so that we can also define the density of number of interfaces); second, as the percentage of value one in the phase character function  $\chi(x, t)$  equals the percentage of martensite, we can call it the function of the phase fraction  $Z(t)$ .

Moreover, the 30 mm long sample was divided into 50 equal intervals. In each 0.6 mm interval, which is one hundred times of the narrowest observable strip width, the distribution of the phase fraction  $z(x, t)$  and the distribution of the number of interfaces  $n(x, t)$  can be obtained.

### 3.2. Experimental Results and Analysis

#### 3.2.1. Characteristics of the stress: stress plateau and sharp stress drop

Typical superelastic behavior was observed at the testing temperature  $T = 293$  K (Fig.2). Linear elastic deformation occurred at small strain for the austenite ( $\varepsilon < \varepsilon_s \approx 1.48\%$ ) and at large strain for martensite ( $\varepsilon > \varepsilon_f \approx 8.60\%$ ). And the effective Young's modulus is  $E \approx 13$  GPa. During the stress induced martensitic transformation process, while the strain change a lot (from 1.48% to 8.60%), the stress only changed a little bit (compared to the previous austenite stage, only changed from 192 MPa to 205 MPa) and exhibited a stress plateau. In this process, the specimen was a mixture of martensites and austenites, and the austenite phase was gradually transformed into the martensite phase with the increasing strain. Remarkably, in the stress plateau, two obvious sharp stress drops had occurred (shown in Fig.3(f)).

#### 3.2.2. Microstructures evolution: nucleation, mixed nucleation and growth, and merging due to growth

Figures 3(a) to 3(e) show the two distribution functions (the distribution of the number of interfaces  $n(x, t_i)$  and the distribution of the phase fraction  $z(x, t_i)$ ) along the sample length at various strains (void round points shown in Fig.3(f)) during the loading process. In the linear elastic range ( $\varepsilon < \varepsilon_s = 1.48\%$ ), the specimen was in the austenite state with  $n = z = 0$ . A mixed martensite and austenite region did not appear until the stress reached the value of 196.0 MPa and then dropped sharply. It indicates that the martensitic transformation would begin with a sharp stress drop. As shown in Fig.3(a), as the stress dropped to the value of 192.7 MPa, in the interval  $x \in [4.5, 6.6]$  mm, it was found that the number of interfaces was very high while the phase fraction was small ( $< 0.4$ ). It indicated that the formed martensitic strips were very thin, so this period is certainly the nucleation period (where  $x_1 \approx 6$  mm was the first nucleation site). Since the nucleation of martensites needs a nucleation energy which should be provided by the elastic energy, this energy transfer may be the main causes of the stress drop<sup>[13]</sup>.

As the loading proceeded to  $\varepsilon = 2.81\%$  (Fig.3(b)), in the middle of the interval  $x \in [1.8, 10.8]$  mm,  $z(x, t)$  became very high and could even reach 1, while  $n(x, t)$  became very small and could even be 0. It means that the nucleated martensitic strips merged together due to the growth of the thin martensitic strips. However, near the two ends of the interval, martensitic strips appeared with very small  $z(x, t)$  and large  $n(x, t)$ . This indicates that many new thin martensitic strips nucleated close to the existing thick strips. Thus, the characteristics of this period are that the martensitic strips grew up in the middle of the interval, new thin martensitic strips nucleated near the two ends of the interval, and the stress changed very little. We can call it the mixed nucleation and growth period. Thus, multi-interface microstructures were formed in the specimen<sup>[9, 11]</sup>, not just due to the simple widening of the initially nucleated martensitic strips<sup>[12]</sup>. From the crystalline theory, the martensitic transformation causes a shear deformation. In our test, the specimen was loaded in the grips which did not allow any movement in the transverse direction. After the nucleation, a complicated stress field with bending, shearing and so on might form inside the sample<sup>[10]</sup>, and this stress field could make it easier for nucleation near the previous nucleation site than simple widening of existing strips. This complicated stress field should be determined by the boundary constrains of the grips and the orientation of the single crystal specimen. Further studies are needed to clarify the mechanism of the above phenomenon.

As the loading proceeded to  $\varepsilon = 3.01\%$ , another sharp stress drop was observed. Correspondingly, a new site of nucleation ( $x_2 \approx 15$  mm) far away from the previous one was found (Fig.3(c)). This new martensite region would widen with the further loading. The characteristics of the nucleation and growth around  $x_2$  were similar to those around  $x_1$  (Fig.3(d)) and these two martensite regions (region I and region II, as shown in Figs.3(d) and 3(e)) met each other at  $x_{I\ II} = 13$  mm. Upon further loading to the end of the transformation (Fig.3(e)), the thin martensitic strips merged into bigger ones. So this period is the merging period due to growth.

Based on the analysis on the distribution of the number of interfaces and the distribution of the phase fraction along the whole sample at different strain values during the loading process, the characteristics of the microstructure evolution during the transformation were obtained. Those characteristics and the stress-strain curve indicated that the whole sample could be divided into two quasi-independent parts during the martensitic transformation process. In each part, the evolution can be divided into three

periods: nucleation of thin martensitic strips accompanied with the stress drop, mixed nucleation and growth period, and merging due to growth which caused the number of interfaces to decrease quickly.

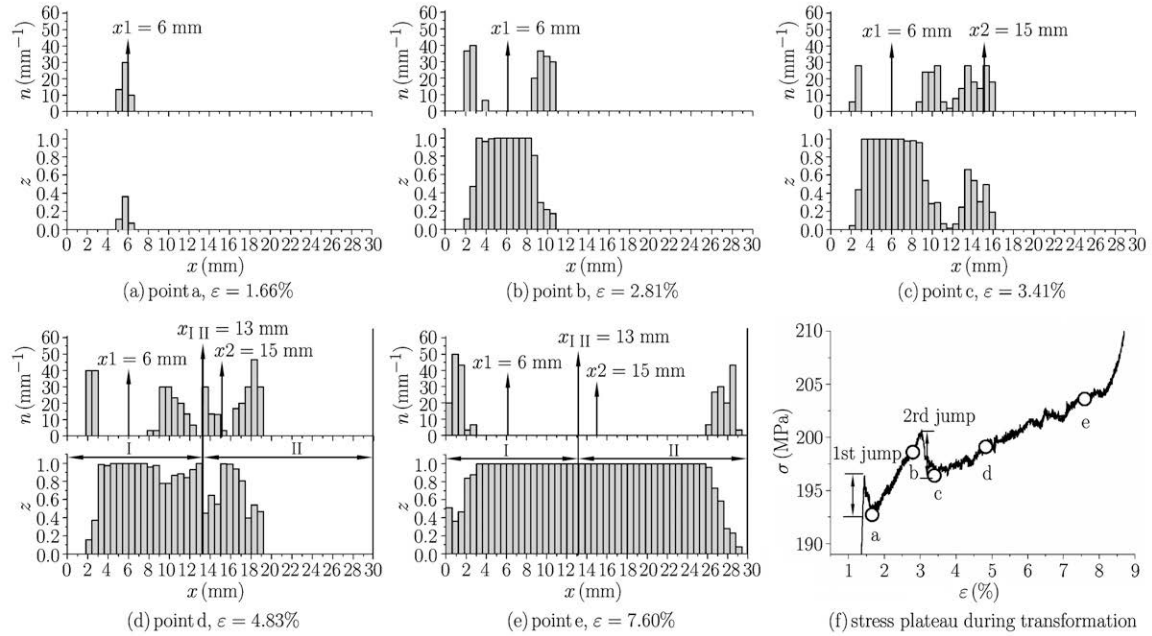


Fig. 3. Microstructures evolution and stress plateau during the transformation process.

3.2.3. Three-period and multi-stage characteristics of the transformation

In order to clarify the characteristics mentioned above, the sample was divided into two parts at  $x_{I\ II} = 13$  mm (where the two regions met and merged), and then the average number of interfaces  $n_{1,2} = N_{1,2}/L_{1,2}$  and average phase fraction  $Z_{1,2}$  were calculated separately for the two parts. In Fig.4, the void round points and solid square points show the experimental results of  $n - Z$  in the two regions, respectively. Obviously, the  $n - Z$  relations in these two regions are very much alike, that all exhibited the three-period characters of the martensitic transformation: nucleation, mixed nucleation and growth, and merging due to growth. Also, the experimental results agreed with the theoretical prediction (Eq.(5)) very well (solid line in Fig.4).

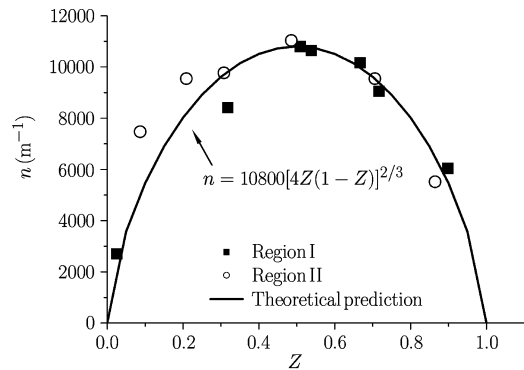


Fig. 4 Average number of interfaces  $n$  as function of the average phase fraction  $Z$ .

The fitted result  $n_{max} = 10800 \text{ m}^{-1}$  show that the maximum numbers of interfaces in the two parts (the length of them are 13 mm and 17 mm) reached 140 and 184. So in this case the coefficient of inhomogeneous energy  $\beta$  should be quite high, which may due to the coupled effect of the restriction of the grips and the shear deformation of martensite in this orientation.

From the above analysis, it seems that the specimen can be considered as two quasi-independent parts and the transformation process in each part was very similar. Therefore the transformation in the whole specimen has the characteristics of multi-stage (two stages here). Multi-stage nucleation and growth process was identified for all the 6 samples under testing. The above three periods of the nucleation and growth process occurred quasi-independently in three (2 samples) or two (4 samples) regions of the specimen. The multi-stage characteristics have not been reported in literatures as far as we know. It might be due to the inhomogeneity induced by local defects and/or interior stresses,

etc. Moreover, the complicated stress state induced by the nucleated martensitic strips might intensify this inhomogeneity. Another possible reason is that the transformation process should be considered as dynamic and the temperature field might also be inhomogeneous. However, these should not be the major reason since the loading rate was very low.

#### IV. CONCLUSIONS

Through the macro stress-strain curve and quantitative analysis of the microstructure evolution process of the CuAlNi single crystal under the uniaxial tension, it was found that the stress-induced martensitic transformation process consisted of three periods: nucleation, mixed nucleation and growth, merging due to growth. The characteristics of the stress, the number of interfaces and the phase fraction were different in each period. During the nucleation, the stress dropped sharply and the number of martensitic strips (the number of interfaces) increased very fast while the total width of martensitic strips (the phase fraction) increased slowly. In the mixed nucleation and growth period, both the stress and the number of martensitic strips (the number of interfaces) changed very little but the total width of martensitic strips (the phase fraction) increased dramatically. Finally in the growth period, the stress and the total width of martensitic strips (the phase fraction) changed slowly while the number of martensitic strips (the number of interfaces) decreased quickly.

The above observations agree quite well with the characteristics of nucleation and growth obtained by the minimization of the energy function under the small parameter approximation. It also indicated that the inhomogeneous energy might have close relationship to the boundary restrictions in the experiment.

Moreover, through the study of the distributions of the number of interfaces and the phase fraction along the whole sample during the transformation, the characteristics of multi-stage was identified. On one hand, many obvious stress drops could be observed in the stress-strain curve; on the other hand, the sample could be considered as several quasi-independent parts and in each part the three-period transformation would occur. Nucleation was accompanied with a stress drop, and the relation between the average interface number and the average phase fraction are similar to and agreed quite well with the theoretical prediction. The reason and its affecting factors need further theoretical and experimental studies.

#### References

- [1] Yang,K. and Gu,C.L., Research and application of the shape memory alloy. *Metallic Functional*, 2000, 17(15): 7-12.
- [2] Dominiek,R. and Hendrik,V.B., Design aspects of shape memory actuators. *Mechatronics*, 1998, 8(6): 635-656.
- [3] Gao,Z.G., Application of the shape memory alloys. *Modern Manufacturing Technology and Equipment*, 2007, 1: 44-45.
- [4] Geng,B., Review on the research status and applied characters of shape memory alloy and its applied character. *Journal of Liaoning University (Natural Sciences Edition)*, 2007, 34(3): 225-228.
- [5] Otsuka,K. and Wayman,C.M., Shape Memory Alloys. Cambridge: Cambridge University Press, 1998.
- [6] Zhang,L., Xie,C.Y. and Wu,J.S., Progress in research on shape memory alloy films in MEMS field. *Materials Review*, 2006, 2: 109-113.
- [7] Bhattacharya,K. and James,R.D., A theory of thin films of martensitic materials with applications to microactuators. *Journal of the Mechanics & Physics of Solids*, 1999, 47: 531-576.
- [8] Xu,Z.Y., Martensitic Transformation and Martensite. Beijing: Science Press, 1980.
- [9] Fang,D.N., Lu,W. and Hwang,K.C., Pseudoelastic behavior of a CuAlNi single crystal under uniaxial loading. *Metallurgical and Materials Transactions A*, 1999, 30: 1933-1943.
- [10] Shield,T.W., Orientation dependence of the pseudoelastic behavior of single crystal of Cu-Al-Ni in tension. *Journal of the Mechanics & Physics of Solids*, 1995, 43: 869-895.
- [11] Otsuka,K., Wayman,C.M., Nakai,K., Sakamoto,H. and Shimizu,K., Superelasticity effects and stress-induced martensitic transformations in Cu-Al-Ni alloys. *Acta materialia*, 1976, 24: 207-226.
- [12] Sun,Q.P., Xu,T.T. and Zhang,X.Y., On deformation of A-M interface in single crystal shape memory alloys and some related issues. *Journal of Engineering Materials and Technology Transactions of the ASME*, 1999, 121(1): 38-43.
- [13] Huo,Y. and Müller,I., Interfacial and inhomogeneity penalties in phase transitions. *Continuum Mechanics and Thermodynamics*, 2003, 15: 395-407.

- [14] Vainchtein,A., Healey,T. and Rosakis,P., Bifurcation and metastability in a new one dimensional model for martensitic phase transitions. *Computer Methods in Applied Mechanics and Engineering*, 1999, 170: 407-421.
- [15] Liu,Q., Ren,J.T., Jiang,J.S. and Guo,Y.Q., An overview of the constitutive model of shape memory alloy and their applications. *Advances in Mechanics*, 2007, 37(2): 189-204.
- [16] Wang,J. and Sheng,Y.P., The development of the constitutive relation of a shape memory alloy. *Chinese Quarterly of Mechanics*, 1998, 19(3): 185-195.
- [17] Seelecke,S. and Mueller,I., Shape memory alloy actuators in smart structures: modeling and simulation. *Applied Mechanics Review*, 2004, 57(1): 27-46.
- [18] Truskinovsky,L. and Zanzotto,G., Ericksen bar revisited: energy wiggles. *Journal of the Mechanics & Physics of Solids*, 1996, 44(8): 1371-1408.
- [19] Huo,Y. and Müller,I., Nonequilibrium thermodynamics of pseudoelasticity. *Continuum Mechanics and Thermodynamics*, 1993, 5: 163-204.
- [20] Huo,Y.Z., Continuum thermodynamical studies on the thermal-elastic martensitic transformation. *Advances in Mechanics*, 2005, 35(3): 305-314.